Journal of Thermal Analysis and Calorimetry, Vol. 93 (2008) 1, 239–245

COMPARATIVE STUDY OF THREE DIFFERENT KINETIC MODELS APPLIED TO THE AGEING OF ARCHAEOLOGICAL BEESWAX USED AS A PAINT MEDIUM

R. Rivenc and M. R. Schilling*

Analytical Technologies Section, The Getty Conservation Institute, http://www.getty.edu/ , 1200 Getty Center Drive, Suite 700 Los Angeles, CA 90049-1684, USA

Kinetic evaluation of thermogravimetry data was used to understand the ageing behavior of beeswax used as an artists' paint medium on ancient mummy shrouds and Fayum portraits. Individual components of beeswax were subjected to dynamic thermogravimetry to assess their evaporation rates, and three methods of kinetic analysis were evaluated for accuracy. The results showed that although it is impossible to accurately predict the volatility at room temperature for individual components of beeswax due mostly to their high molecular mass, relative trends and ranking of the volatility of the compounds can be obtained which may explain compositional changes over time.

Keywords: *beeswax, kinetic evaluations, thermogravimetry*

Introduction

Beeswax has a long history of use as an artists' paint medium, dating back to ancient Egypt where it was used on Fayum portraits and mummy shrouds [1]. Fresh beeswax is composed of alkanes, alkenes, monoesters and fatty acids, plus small fractions of diesters and fatty alcohols [2, 3]. The proportion of the various components varies according to the species of bee. Wax from the common honeybee, *Apis mellifera*, contains 11 to 28% odd-numbered hydrocarbons (C_{23} to C_{31}), 1 to 18% even-numbered free fatty acids, and 26 to 41% esters of palmitic acid with even-numbered fatty alcohols [3]. Heptacosane is, by far, the most abundant hydrocarbon, whereas palmitic acid and tetracosanoic acid are the most abundant fatty acids, and are present in their free and esterified forms [2].

When ancient paints containing beeswax medium are analyzed by gas chromatography/mass spectrometry (GC/MS), the resulting chromatograms differ significantly from those of fresh beeswax [4, 5]. One of the main changes detected by GC/MS is the severe depletion of the alkane fraction. Figure 1 shows an overlay of chromatograms for fresh beeswax and beeswax paint medium from a 1st century A.D. red-shroud mummy in the collections of the J. Paul Getty Museum at the Getty Villa, in Malibu (accession number 91.AP.6). Biological deterioration has been advanced as a possible explanation for the change in composition, but evaporation of the lower molecular mass components of beeswax over time may also be a contributing factor [4].

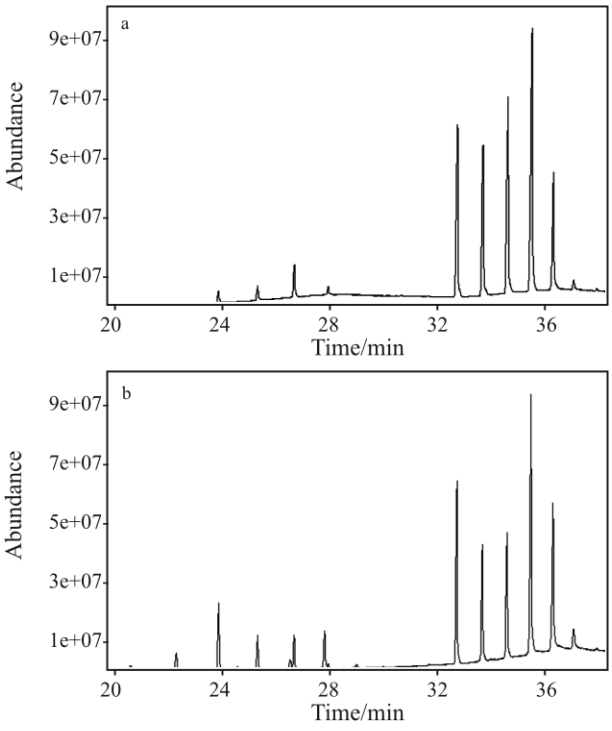

Fig. 1 Chromatograms of a sample from the beeswax found on the red-shroud mummy in the collections of the J. Paul Getty Museum at the a – Getty Villa and b – fresh beeswax

Kinetic evaluation of thermogravimetry data (TG) is routinely used in industry to assess lifetimes of materials, but has seldom been applied in the field of conservation of cultural heritage [6, 7], even

* Author for correspondence: rrivenc@getty.edu

1388–6150/$20.00

Akadémiai Kiadó, Budapest, Hungary
Springer, Dordrecht, The Netherlands

though thermal analysis has a long record of application in the field [7, 8]. One of the obvious difficulties lies in extrapolating predictions based on test results that were obtained at high temperature over a short duration to ambient temperature conditions in sites or museum galleries where objects may remain for centuries. The research presented here explores the possibility of using reaction kinetics to explain compositional changes over time in ancient beeswax paint medium. The main individual components of beeswax – alkanes, fatty acids, alcohols, and a monoester – were studied by TG. The results from three different reaction kinetics models were compared: two are based on n^{th}-order reaction kinetics whereas the third is based on model-free kinetics.

Experimental

Materials

The following standard compounds were used for the thermogravimetric experiments: Alkanes (≥98% purity): eicosane, pentacosane, tritriacontane (Aldrich); heptacosane, nonacosane, hentriacontane, tricosane (Fluka). Fatty acids (all ≥99% purity except where noted): lauric, myristic, palmitic (95%), stearic, eicosanoic, docosanoic; tetracosanoic (Fluka); hexacosanoic, octacosanoic, triacontanoic (Sigma). Alcohols (≥97% purity): tetracosanol, hexacosanol, octacosanol (Sigma). Monoester: palmitic acid behenyl ester** (Sigma, 99% purity). The compounds were used as received.

Methods

Thermogravimetric analysis

A Mettler Toledo TGA/SD TA 851^e instrument was used for the experiments. The instrument was calibrated using a Mettler Toledo total calibration procedure with respect to indium and aluminum standards. Dynamic runs were performed at 5, 10 and 20°C min^{-1} for each standard tested using 70 μL, 4.69 mm i.d. sapphire crucibles with nitrogen purge gas at 50 mL min^{-1}. In the temperature programs, an initial 3 min isothermal segment allowed the furnace to purge with nitrogen, then the temperature was ramped to 600°C at the specified heating rate. In the isothermal runs, performed at various temperatures under nitrogen at 50 mL min^{-1}, the temperature was ramped at 40°C/min until the desired isothermal temperature was reached. Mettler STAR^e software version 8.10 was used to perform n^{th}-order kinetics and model-free kinetics calculations.

Evaluation of three reaction kinetics models

The first model tested was n^{th}-order kinetics, in which the rate of reaction, $d\alpha/dt$, is defined as a function of conversion, α, and the rate constant, k, by the following equation:

$$d\alpha/dt=kf(\alpha) \quad (1)$$

The temperature dependence of the rate constant is expressed by the Arrhenius equation:

$$k_T=k_0^{-E_a/RT} \quad (2)$$

where T is the absolute temperature in K, k_T is the rate constant at temperature T, k_0 is the rate constant at infinite temperature (also known as the pre-exponential factor), E_a is the activation energy, and R is the universal gas constant.

By substituting k with the Arrhenius equation as shown in Eq. (2), Eq. (1) may be rewritten as:

$$d\alpha/dt=k_0^{-E_a/RT}f(\alpha) \quad (3)$$

When an n^{th}-order model is assumed, $f(\alpha)=(1-\alpha)^n$ and Eq. (3) becomes:

$$d\alpha/dt=k_0^{-E_a/RT}(1-\alpha)^n \quad (4)$$

In the case of TG experiments, $d\alpha/dt$ is the normalized DTG curve. The STAR^e software uses multiple linear regression to calculate E_a, k_0 and n (the order of the reaction) from a set of TG curves acquired with three or more heating rates.

The second model evaluated was best described in a series of papers by Dollimore *et al.* for studying the volatility of small molecules by focusing on the rising temperature portion of DTG curves [9–17]. It is based on the assumption that, given a constant evaporative surface area, evaporation obeys a zero-order reaction for which n=0 in Eq. (4). The shape of the DTG curve is indicative of whether or not the evaporation of a given substance is truly zero-order, as shown in Fig. 2. For zero-order reactions, Eq. (4) is integrated to yield the simplified rate equation:

$$A=A_0-kt \quad (5)$$

where A_0 is the amount of starting material, and A is the amount remaining at time t. The other important kinetic data are obtained from the Arrhenius equation, which may be rewritten as:

$$\ln k_T=\ln k_0-E_a/RT \quad (6)$$

** Palmitic acid behenyl ester is not actually found in beeswax where all the esters have higher carbon numbers, starting from C40, but it is commercially available as a chemical standard and was used as indicative of the behavior of monoesters.

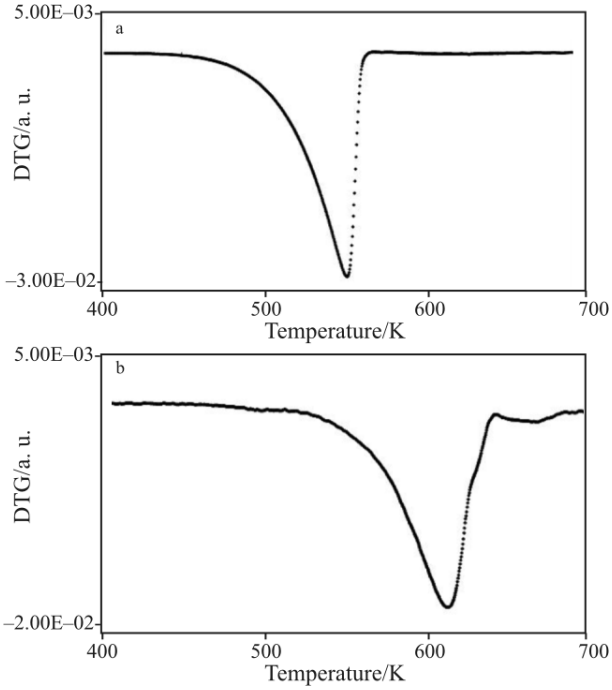

Fig. 2 The normalized DTG curve of a – palmitic acid exhibits zero-order behavior, b – tetracosanoic acid shows that evaporation does not follow zero-order kinetics. Heating rate: 20°C min^{-1}

The slope of this plot is the activation energy, E_a, and the intercept is the pre-exponential factor, $\ln k_0$.

Dollimore's procedure also makes it possible to estimate properties that often must be considered when assessing material performance, such as vapor pressure, volatilization rate, and enthalpy of vaporization. To begin, because the vapor pressure of a material is directly proportional to temperature, the Antoine Eq. (7) may be used to calculate the vapor pressure of a compound based on a set of three constants (A, B and C), which are valid only within a specified temperature range.

$$\log P = A - B/(T+C) \quad (7)$$

Antoine constants are published for many types of compounds [18]. However, for compounds with unknown Antoine constants, the Langmuir equation may be used instead to calculate vapor pressure. The Langmuir equation expresses the relationship between vapor pressure and the rate of volatilization:

$$P = [\alpha^{-1}(2\pi R)^{1/2}][(T/M)^{1/2}(dm/dt)] \quad (8)$$

where P is the vapor pressure in Pascals, dm/dt is the rate of volatilization (calculated by dividing the DTG data in kg s^{-1} by the cross-sectional area of the crucible in m^2), T the absolute temperature, R is the universal gas constant (8.314 J mol^{-1} K^{-1}), M the molecular mass of the compound evaporating into the vapor phase (in kg mol^{-1}), and α is the vaporization constant (taken as unity in vacuum). In the presence of a purge gas, as in thermogravimetry experiments, α cannot be assumed to be unity but instead must be calculated. This is achieved by rewriting the equation as:

$$P = k_{evap}\nu \quad (9)$$

where $\nu=(T/M)^{1/2}(dm/dt)$ and $k_{evap}=\alpha^{-1}(2\pi R)^{1/2}$. ν is a constant for a given set of experiments, provided that a container with a constant surface area is used.

k_{evap}, the coefficient of evaporation, is the key factor as it does not depend on the compound studied but on factors such as the surface area of evaporation, the universal gas constant, and the vaporization coefficient. k_{evap} can be calculated for a compound with published Antoine constants, then subsequently used to construct vapor pressure plots for compounds with unknown Antoine constants. Non-linear regression analysis may be used to determine the Antoine constants from the vapor pressure plots.

The enthalpy of vaporization of the compounds studied may also be determined from the vapor pressure by way of the Clausius–Clapeyron equation:

$$\log P = [\Delta H_{vap}/(2.303R)][1/T] \quad (10)$$

A plot of $\log P$ *vs.* $1/T$ generates ΔH_{vap} values for the compounds under consideration.

Therefore, by following Dollimore's procedure, it is possible to obtain vapor pressure plots, rate of volatilization, and the enthalpy of vaporization to characterize the volatility of compounds and permit their ranking. However, the procedure is subject to a number of limitations. Because Antoine constants are valid only within a limited temperature range, the value of k_{evap} derived for a compound from its Antoine constants is valid only within the same temperature range. k_{evap} also varies with ν, which is a function of temperature. However, it has been demonstrated by Tatavarti *et al.* [16] that the variation is minimal. The same researchers also demonstrated that k_{evap} calculated for a type of compound could validly be used to calculate the vapor pressure plots of chemically-different compounds [16].

The third method tested in this paper is the model-free kinetics (MFK) evaluation in the STAR^e software. Automated calculations provide E_a as a function of conversion. The Arrhenius equation and the reaction rate equation are integrated in a way that eliminates the need to know the reaction order, n.

Results and discussion

As described above, the zero-order method provides a number of parameters for assessing the volatility of

Table 1 Antoine constants range and k_{evap} values obtained at 20°C min^{-1} for alkanes and fatty acids

Compound	Antoine constants range: *T* low/K	Antoine constants range: *T* high/K	k_{evap} 20°C min^{-1}
Alkanes			
Pentacosane	457	675	124731
Heptacosane	473	695	144899
Nonacosane	488	714	137430
Hentriacontane	503	732	137185
Tritriacontane	517	749	
	Upper limit *T* low/K	Lower limit *T* low/K	Average
	517	675	136061
Fatty acids			
Lauric acid	393	573	128877
Myristic acid	423	599	121077
Palmitic acid	440	625	123951
Stearic acid	457	649	137430
Eicosanoic acid	477	670	125924
Docosanoic acid	373	600	139376
Tetracosanoic acid	483	536	141105
	Upper limit *T* low/K	Lower limit *T* low/K	Average
	483	536	131105

compounds. It was possible to derive k_{evap} values directly for compounds with published Antoine constants. The values of k_{evap} obtained were fairly consistent with some variations depending on the class of compound and the heating rate. It was observed that values calculated from the TG runs performed at 20°C min^{-1} show better agreement (cf. Table 1).

For compounds with unknown Antoine constants, the rate of volatilization (d*m*/d*t*) and vapor pressure (*P*) were calculated by substituting a suitable mean value for k_{evap} into Eq. (9). The upper and lower temperature limits over which the mean k_{evap} value is valid were established by the maximum temperature from the lower limits of the set of individual compounds, and the minimum temperature of the upper limits.

The validity of the method is confirmed by the agreement between vapor pressure plots calculated from Antoine constants *vs.* those calculated from the mean k_{evap} values. This process also shows that compounds with high carbon numbers, especially those that can hydrogen-bond in the vapor phase, tend not to exhibit truly zero-order behavior. In this case, discrepancies appear between the two methods of calculating vapor pressure (Fig. 3). Of the compounds tested, alkanes above C_{31}, fatty acids above C_{24}, and fatty alcohols exhibit non zero-order behavior, hence could not be assessed with Dollimore's method. For compounds with functional groups susceptible to dimerization in the vapor phase, Tatavarti's suggestion [16] of using the corrected molecular mass of associated dimers rather than of the monomer to calculate ν did not improve the present results. It is possible that only a fraction of the molecules exist as dimers in vapor phase, so that assuming complete dimerization also leads to inaccurate results.

Trends confirm, as expected, that volatility decreases as the number of carbons increases. Functional groups also play an important role in reducing volatility. Figure 4 illustrates the variations in the activation energy and the enthalpy of vaporization*** *vs.* carbon number. Vapor pressure plots obtained from Antoine constants exhibit similar trends (Fig. 5). Errors in the calculation of ΔH_{vap} originate from k_{evap} and represents approximately 6% of the averaged value. The agreement between the ΔH_{vap} estimates for alkanes and a linear curve fitted to published ΔH_{vap} data [19] is within ±10%. Errors in E_a are harder to quantify as they strongly depend on the portion of the DTG curve selected for assessment.

The ranking of compounds according to their rate of volatilization d*m*/d*t* (Fig. 6) shows palmitic acid is far more volatile than pentacosane. While these trends are consistent with the depletion of the alkane fraction in beeswax observed in the chromato-

*** Different methods, calculated or experimental, of estimating the enthalpy of vaporization exist. It is accepted that the results would show slight variations depending on the method used.

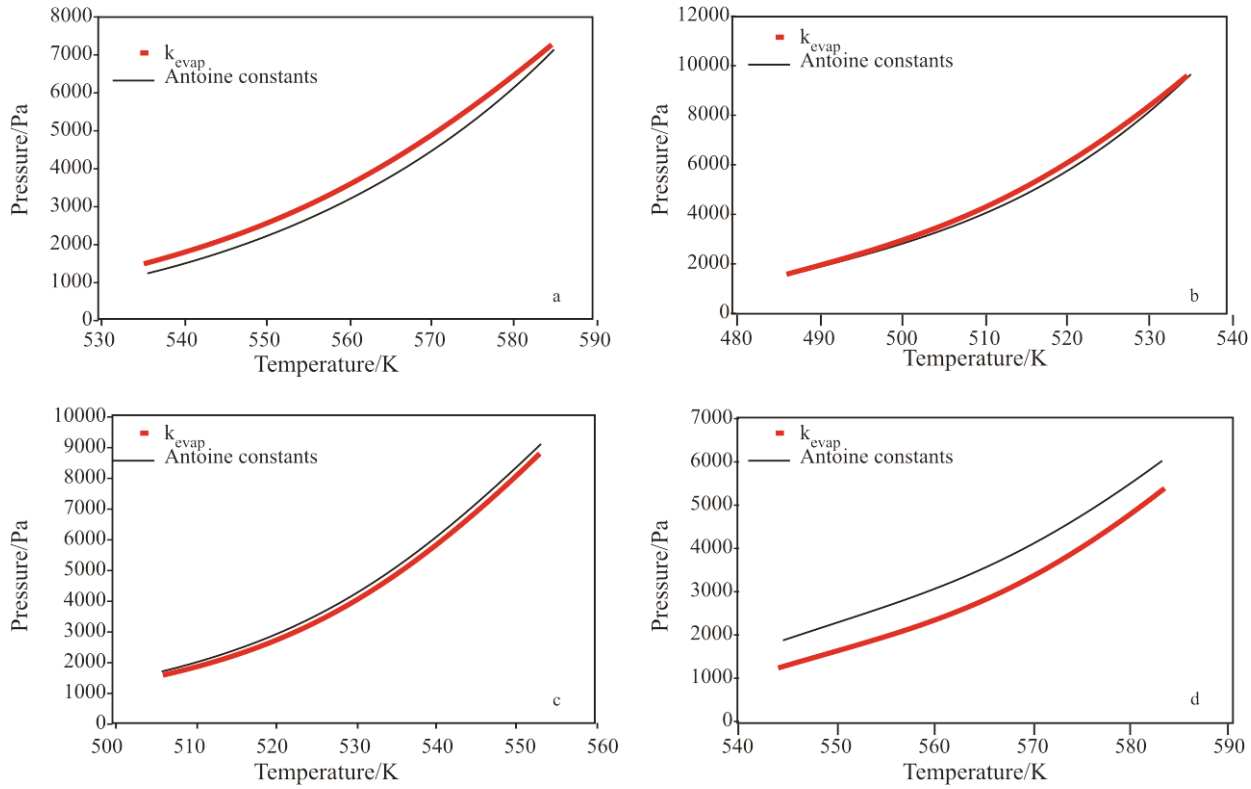

Fig. 3 Vapor pressure plots calculated with k_{evap} and from Antoine constants; a – heptacosane, b – palmitic and c – stearic acids plots show very good agreement while d – tetracosanoic acids show discrepancies

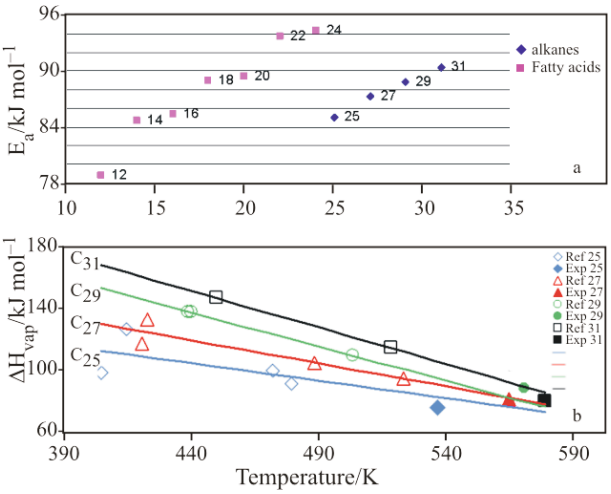

Fig. 4 a – E_a of alkanes and fatty acids and b – ΔH_{vap} of alkanes, compared to published reference data (Chickos and Acree, Jr. 2003)

gram of the paint sample from the mummy shroud, they also suggest that smaller fatty acids such as palmitic acid should have evaporated faster than the alkane fraction. This is however not the case as palmitic acid is still very abundant in the aged beeswax. Two main reasons can explain this: wax monoesters are likely to undergo hydrolysis to release additional free palmitic acid, and free fatty acids are likely

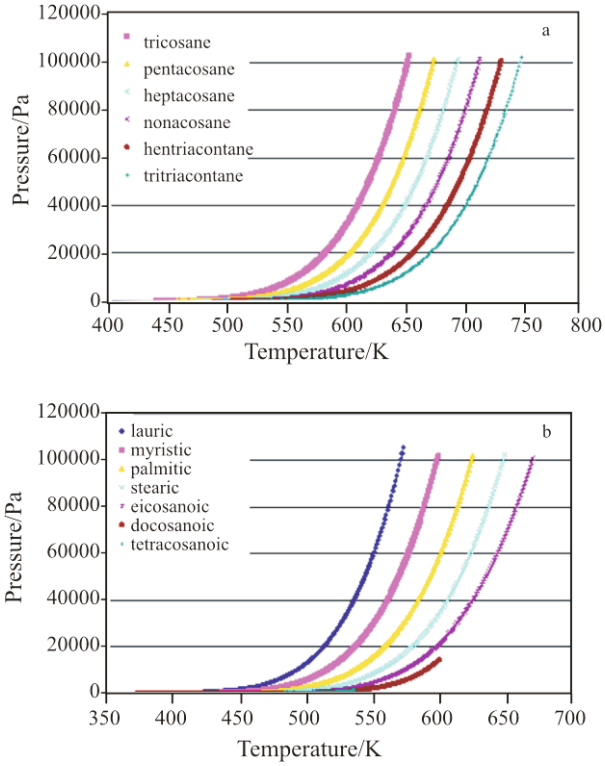

Fig. 5 Vapor pressure plots calculated with Antoine constants for a – alkanes and b – fatty acids

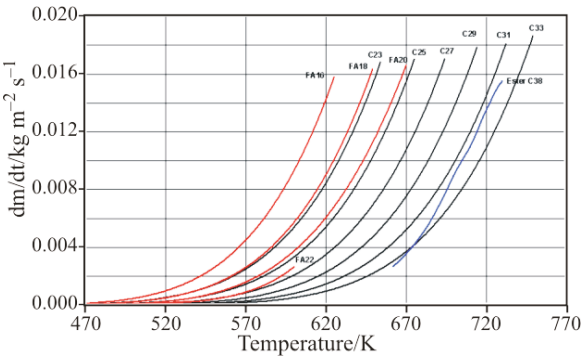

Fig. 6 Rate of volatilization d*m*/d*t* of alkanes (C23, C25, C27, C29, C31 and C33 in black) and fatty acids (FA16, FA18, FA20 and FA22 in red) plotted *vs.* temperature

Table 2 Comparisons of predictions for the time in minutes to reach 10% conversion based on the three different kinetic methods with actual results from isothermal tests

Compound	*T*/min for 0.1 conversion				
	T/K	MFK	n^{th} order	Zero order	Isothermal run
Pentacosane	447	29.3	60*	14.7	29.3
	557	–	0.5	0.2	0.4
Heptacosane	494	10.1	11.4*	3.1	11.6
	547	–	1.2	0.4	1.6
Nonacosane	473	53.7	66*	14.0	45.3
	528	–	4.7	1.3	5.0
Palmitic acid	526	–	0.4	0.1	0.4
	531	0.3	0.6*	0.1	0.4
Tetracosanoic acid	507	16.4	25.2*	3.8	17.1
	559	–	1.5	0.5	1.6

*predictions based on manual calculations using the kinetic data provided by STAR^e software

to form metal carboxylates or metal soaps with the red lead pigment present in the paint from the mummy shroud. Unlike the fatty acids in beeswax, some metal soaps are stable above 630 K, hence are unlikely to evaporate significantly from the film.

Predictions of evaporation rate made from the zero-order model were found to be less accurate than those from n^{th}-order and model-free kinetics. For example, Table 2 compares the results of actual isothermal tests to achieve 10% conversion with the predictions based on the three different methods. MFK and n^{th}-order predictions show good agreement with data from the isothermal tests, whereas predictions based on the zero-order method systematically overestimated the volatility of the compounds tested. It is also recommended that predictions are not extrapolated 50 degrees beyond the mass-loss step. Figure 7 illustrates the discrepancy between predictions based

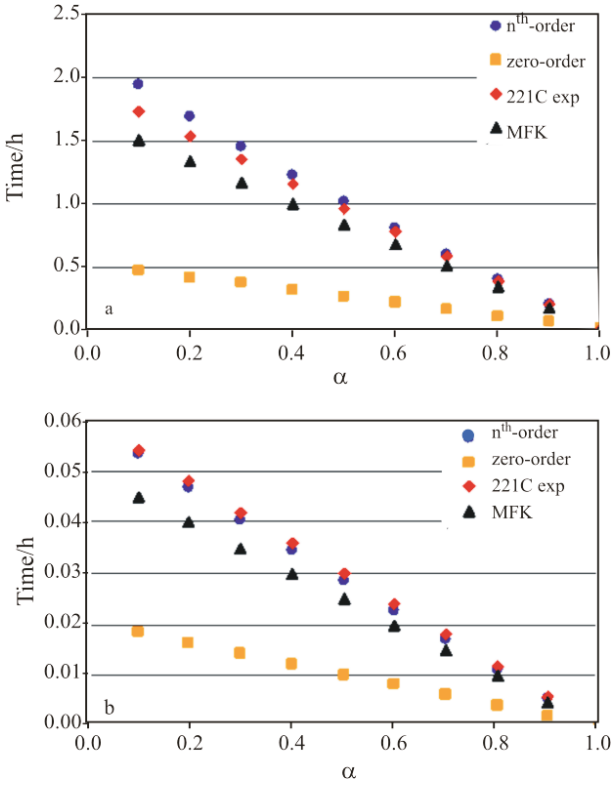

Fig. 7 Conversion plotted of a – heptacosane, b – palmitic acid *vs.* time according to isothermal runs, n^{th}-order, zero-order and MFK predictions

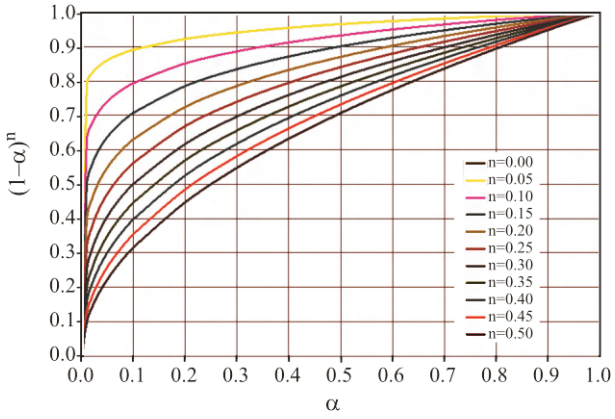

Fig. 8 $(1-\alpha)^n$ plotted *vs.* conversion showing the effect of *n* on conversion curves

on a zero-order model of reaction and n^{th}-order predictions as well as isothermal runs for heptacosane and palmitic acid. The greater accuracy of n^{th}-order *vs.* zero-order predictions is probably due to the fact that, especially for larger molecules, the evaporation process cannot be assumed to be zero-order throughout its entire duration. The effect of *n* on isothermal conversion curves is shown in Fig. 8.

Conclusions

In the present study, the depletion of the alkane fraction in the chromatogram of aged beeswax is consistent with their greater volatility compared to the higher molecular mass components such as wax esters. Evaporation undoubtedly affects the composition of ancient beeswax in works of art that have been stored in museums for extremely long periods of time. However, the absolute rates of evaporation of individual components in beeswax used in works of art cannot be predicted with high accuracy because the temperatures in museums lie far below the temperature range of the mass loss steps of the individual components, and because phase changes also alter evaporation rates. Although the zero-order kinetic model was less than successful in predicting the behavior of beeswax components in isothermal aging studies, the combination of Antoine and Langmuir equations retains its validity, and all three models tested provided consistent relative trends for classes of components.

References

1 J. S. Mills and R. White, The Organic Chemistry of Museum Objects, 2nd Ed., Butterworth-Heinemann, Oxford 1994, p. 49.
2 J. J. Jimenez, J. L. Bernal, S. Aumente, M[a]. J. del Nozal, M[a]. T. Martin and J. Bernal Jr., J. Chrom. A, 1024 (2004) 147.
3 R. Aichholz and E. Lorbeer, J. Chrom. A, 855 (1999) 603.
4 M. Regert, S. Colinart, L. Degrand and O. Decavallas, Archaeometry, 43 (2001) 551.
5 M. R. Schilling and J. Mazurek, unpublished results.
6 M. Schilling, D. Carson and H. Khanjian, ICOM Committee for Conservation Preprints, 12th triennial meeting, Lyon, 29 August–3 September 1999, J. Bridgland, Ed., (London: James and James), France 1999, pp. 242–247.
7 B. Roduit and M. Odlyha, J. Therm. Anal. Cal., 85 (2006) 157.
8 J. Pires and A. J. Cruz, J. Therm. Anal. Cal., 87 (2007) 411.
9 D. M. Price and M. Hawkins, Thermochim. Acta, 315 (1998) 19.
10 S. Lerdkanchanaporn and D. Dollimore, Thermochim. Acta, 324 (1998) 15.
11 D. Dollimore and C. O'Connell, Thermochim. Acta, 324 (1998), 33.
12 K. Chatterjee, D. Dollimore and K. Alexander, Int. J. Pharm., 213 (2001) 31.
13 K. Chatterjee, D. Dollimore and K. Alexander, Thermochim. Acta, 392–393 (2002) 107.
14 L. Burnham, D. Dollimore and K. S. Alexander, Thermochim. Acta, 392–393 (2002), 127.
15 P. Phang, D. Dollimore and S. J. Evans, Thermochim. Acta, 392–393 (2002) 119.
16 A. Tatavarti, D. Dollimore and K. Alexander, J. Amer. Assoc. Pharm. Sci., 4 (2002) 1.
17 S. F. Wright, D. Dollimore, J. G. Dunn and K. Alexander, Thermochim. Acta, 421 (2004) 24.
18 R. M.Stephenson and S. Malanowski, Handbook of the Thermodynamics of Organic Compounds, Elsevier, New York 1967.
19 J. S. Chickos and W. E. Acree, Jr., J. Phys. Chem. Ref. Data, 32 (2003) 519.

DOI: 10.1007/s10973-007-8701-8